Avances en Biomedicina
Publicación Oficial del Instituto de Inmunología Clínica
Mérida-Venezuela
Volumen 14(2), Julio-Diciembre 2025, p 149-160
Copyright: © ULA 2025
Depósito Legal: PPI201102ME3935
ISSN: 2477-9369
PII: S2477-9369(25)14019-O
https://doi.org/10.53766/AVANBIO/2025.14.2.08.

Multi-dimensional assessment of tumor hypoxia, survival outcomes, and molecular stratification in breast cancer using computational skills

(Evaluación multidimensional de la hipoxia tumoral, los resultados de supervivencia y la estratificación molecular en el cáncer de mama mediante habilidades computacionales)

Emmanuel M Migabo[1,5] ✉, Tat'y Mwata-Velu[2,5], Richard Mavuela-Maniansa [5], Rachel Milomba Velu [3], Blaise Tshibangu-Mbuebue [4], Blaise Angoma-Shindani [5], Noor Yaseen [6], Aidor Mbungu Baptista [7]

[1] Department of Electrical Engineering, Tshwane University of Technology, Staatsartillerie Rd, Pretoria 0001, Private Bag X680, Gauteng, South Africa.

[2] Departments of Electrical Engineering and Computer Science, Institute Supérieur Pedagogique Technique de Kinshasa, Avenue de la science n°5, Gombe, Kinshasa, 01204, Democratic Republic of the Congo.

[3] Centro de Investigación en Computación, Instituto Politécnico Nacional (CIC- IPN), Avenida Juan de Dios Bátiz esquina Miguel Othón de Mendizábal Colonia Nueva Industrial, Vallejo, Gustavo A. Madero, Ciudad de México, CP 07738, Ciudad de México, México.

[4] Instituto Politécnico Nacional, Escuela Nacional de Ciencias Biológicas, Laboratorio de Micología, Plan de Ayala y Carpio s/n, Sto. Tomás, Alcaldía Miguel Hidalgo, CP 11340, Ciudad de México, México

[5] School of Medicine, Cavendish University Zambia, Longacres Campus, situated at Plot No. 20842, Off Alick Nkata Road, Lusaka, P.O. Box 34625, Zambia.

[6] Departamento de Electrónica, Instituto Nacional de Astrofísica, Óptica y Electrónica, Calle Luis Enrique Erro No. 1, Tonantzintla, Puebla, 72840, Ciudad de México, México.

[7] Department of Mathematics and Computing, Université Pédagogique Nationale (UPN), Route de Matadi Avenue de la Libération (ex-24 Novembre), Quartier Binza/UPN, Commune de Ngaliema, Kinshasa, Kinshasa, B.P. 8815, Democratic Republic of the Congo.

Received: 10th August 2025
Accepted: 11th September 2025.
Online publication: 9rd October 2025.

[ORIGINAL PAPER]

PII: S2477-9369(25)14019-O

Abstract(english)

✉ **Correspondence author:** Dr. Emmanuel M. Migabo. Department of Electrical Engineering, Tshwane University of Technology, Staatsartillerie Rd, Pretoria 0001, Private, Bag X680, Gauteng, South Africa. Email: MigaboME@tut.ac.za.

Tumor hypoxia plays a critical role in cancer progression and treatment resistance, and gene expression-based scoring systems such as Buffa, Ragnum, and Winter have been developed to quantify hypoxia levels. Under- standing the relationship between hypoxia, survival outcomes, and clinical stratifiers like molecular subtype and race is essential for advancing person- alized care in breast cancer. Hypoxia scores were analyzed across tumor stages using Buffa, Ragnum, and Winter models. Kaplan-Meier survival analysis evaluated the prognostic impact of high versus low Buffa scores on progression-free survival (PFS), disease-free survival (DFS), and disease-specific survival (DSS). Stratified analyses were conducted by molecular subtype, AJCC stage, and race. Pearson correlation measured concordance among hypoxia scores. Microsatellite instability (MSI) was assessed using MANTIS and MSI Sensor scores, and their association with genomic instability (Fraction Genome Altered) was explored. Buffa and Winter scores revealed higher hypoxia in inter- mediate stages (IIA, IIB), whereas Ragnum showed more uniform levels. Elevated Buffa scores were significantly associated with worse PFS, DFS, and DSS. Lumi- nal A subtype had better prognosis than Basal-like and Luminal B; advanced stages and Black or African American patients showed poorer outcomes. Strong correlations were found among hypoxia scores (r = 0.65–0.88). Most tumors were microsatellite stable, but a subset with high MSI Sensor scores also showed increased genomic alterations. Hypoxia levels vary by stage and scoring system and are strongly linked to survival outcomes. Molecular subtype, tumor stage, and race significantly affect prognosis, emphasizing the need for multidimensional stratification. Hypoxia scores are concordant and useful, and MSI may contribute to genomic instability in specific subgroups of breast cancer.

Keywords(english)

Hypoxia, Breast Cancer, Buffa Score, Survival Analysis, Molecular Subtypes, Tumor Stage, Race, MSI, Genomic Instability.

Resumen(español)

La hipoxia tumoral desempeña un papel fundamental en la progresión del cáncer y la resistencia al tratamiento, y se han desarrollado sistemas de puntuación basados en la expresión génica como Buffa, Ragnum y Winter para cuantificar los niveles de hipoxia. Comprender la relación entre la hipoxia, los resultados de supervivencia y los estratificadores clínicos como el subtipo molecular y la raza es esencial para avanzar en la atención personalizada en el cáncer de mama. Las puntuaciones de hipoxia se analizaron en todos los estadios tumorales utilizando los modelos Buffa, Ragnum y Winter. El análisis de supervivencia de Kaplan-Meier evaluó el impacto pronóstico de las puntuaciones Buffa altas frente a bajas en la supervivencia libre de progresión (SLP), la supervivencia libre de enfermedad (SSE) y la supervivencia específica de la enfermedad (SEE). Se realizaron análisis estratificados por subtipo molecular, estadio AJCC y raza. La correlación de Pearson midió la concordancia entre las puntuaciones de hipoxia. La inestabilidad de microsatélites (MSI) se evaluó utilizando las puntuaciones MANTIS y MSI Sensor, y se exploró su asociación con la inestabilidad genómica (fracción del genoma alterado). Las puntuaciones de Buffa y Winter revelaron mayor hipoxia en estadios intermedios (IIA, IIB), mientras que Ragnum mostró niveles más uniformes. Las puntuaciones elevadas de Buffa se asociaron significativamente con peores PFS, DFS y DSS. El subtipo luminal A tuvo mejor pronóstico que Basal-like y Luminal B; los pacientes en estadios avanzados y de raza negra o afroamericana mostraron peores resultados. Se encontraron fuertes correlaciones entre las puntuaciones de hipoxia (r = 0,65–0,88). La mayoría de los tumores eran microsatélites estables, pero un subconjunto con puntuaciones altas del sensor MSI también mostró mayores alteraciones genómicas. Los niveles de hipoxia varían según el estadio y el sistema de puntuación y están fuertemente vinculados a los resultados de supervivencia. El subtipo molecular, el estadio del tumor y la raza afectan significativamente el pronóstico, lo que enfatiza la necesidad de una estratificación multidimensional. Las puntuaciones de hipoxia son concordantes y útiles, y el MSI puede contribuir a la inestabilidad genómica en subgrupos específicos de cáncer de mama.

Palabras clave(español)

Hipoxia, cáncer de mama, índice de Buffa, análisis de supervivencia, subtipos moleculares, estadio tumoral, raza, MSI, inestabilidad genómica.

Introduction

Hypoxia is a hallmark of the tumor microenvironment [1] that arises due to an imbal- ance between oxygen supply and consumption [2]. In solid tumors, particularly breast cancer, hypoxia plays a pivotal role in driving tumor progression [3], angiogenesis [3, 4], immune evasion [5], and therapeutic resistance [6]. As a result, it has emerged as both a prognostic indicator and a potential therapeutic target. Quantifying hypoxia through gene expression-based scoring systems has enabled researchers to evaluate tumor oxygenation indirectly, offering insights into the biological aggressiveness of individual tumors [7]. While multiple hypoxia gene expression signatures (Buffa, Rag- num, Winter) have been developed to

quantify this critical microenvironmental feature [8], their prognostic utility and consistency across tumor stages remain poorly charac- terized. These signatures leverage different sets of oxygen-responsive genes to classify tumors based on their transcriptional hypoxic [9–11] states. Despite their widespread use, the degree to which these scoring systems concur, especially across tumor stages and clinical subgroups, remains underexplored. Furthermore, the prognostic relevance of these hypoxia metrics in relation to survival outcomes and how they correlate with known clinical variables such as molecular subtype and race have yet to be fully delin- eated in large breast cancer cohorts. Hypoxia is not only relevant in cancer, where it may further affect TP53 a key gene involved in many cancers [12, 13] but it also plays an important role in testosterone and insulin regulation [14–16], which is itself critical in other serious diseases such as diabetes and cardiovascular complications under hormonal fluctuations [17–21]. This study addresses these questions by evalu- ating hypoxia dynamics [22, 23] across tumor stages, assessing the prognostic utility of the Buffa hypoxia score, and examining survival stratification by clinical features such as tumor stage, race, and molecular subtype. The dynamics of hypoxia can be significantly influenced by the use of medicinal herbs [24–27] as earlier reported but not tested. We also assess the concordance among hypoxia scoring systems and inves- tigate their relationship with genomic instability, particularly microsatellite instability (MSI). Through this integrative approach, we aim to deepen the understanding of how hypoxia influences tumor behavior and outcomes in breast cancer.

Materials and methods

Data Collection and Preprocessing. We utilized clinical and genomic data from The Cancer Genome Atlas (TCGA) Pan- Cancer Atlas project, specifically focusing on patients diagnosed with breast invasive carcinoma (BRCA). The dataset was downloaded from the cBioPortal platform and comprised clinical records for 500 patients. Key clinical variables included patient age, race, tumor subtype, AJCC pathological tumor stage, and follow-up data for survival endpoints such as progression-free survival (PFS), disease-free survival (DFS), and disease-specific survival (DSS). Molecular features such as the BUFFA hypoxia score, mutation count, and aneuploidy score were also included for integrative analysis. After preprocessing and removal of incomplete records, the final cohort size varied slightly across survival types depending on data availability. To ensure consistency in time-to-event analysis, all survival time variables were expressed in months, and status indicators were binary-coded, with 1 representing an event (e.g., progression, recurrence, or disease-specific death) and 0 indicating censoring.

Survival Analysis Using Kaplan–Meier Estimation. We conducted Kaplan–Meier survival analysis to visualize and compare survival out- comes across different clinical and molecular subgroups. The KaplanMeierFitter class from the lifelines Python library was used for this purpose. Tumor Subtype: Patients were grouped by molecular subtype (e.g., Luminal A, Luminal B, HER2-enriched, Basal-like), and survival functions for PFS, DFS, and DSS were compared among these subtypes. AJCC Pathological Tumor Stage: Stratification was based on tumor stage (e.g., Stage I, II, III, IV), evaluating stage-specific survival trends. Race: We explored racial disparities in survival by analyzing groups such as White, Black or African Amer- ican, Asian, and others. BUFFA Hypoxia Score: The hypoxia score was dichotomized using the cohort median into High and Low categories to assess its impact on prog-nosis. Age Group: Patients were classified into three age brackets: < 50, 50–65, and > 65 years. This stratification was used to examine age-related survival differences. For each group comparison, Kaplan–Meier curves were plotted with survival proba- bilities on the y-axis and time in months on the x-axis. Confidence intervals were not displayed to improve visual clarity. The plots included group-specific legends and were standardized in size and formatting using matplotlib.

Cox Proportional Hazards Regression Analysis. To further investigate the effect of specific covariates on progression-free survival, we performed a Cox proportional hazards regression using the CoxPHFitter model from lifelines. The regression model included age, total mutation count, and aneu- ploidy score as explanatory variables. The analysis was performed on 224 patients with complete data, among whom 25 experienced a PFS event. None of the covari-ates demonstrated statistically significant associations with PFS (p-values > 0.05). The hazard ratios (HRs) for age and mutation count were near 1, suggesting negligi-ble influence on the hazard of progression. Aneuploidy score showed a weak negative association (coefficient = −0.01, HR = 0.99), but this effect was also not statistically significant (p = 0.85). Model performance was evaluated using standard metrics: the concordance index (C-index) was 0.47, indicating limited discriminative ability, while the partial AIC was 227.25.

The log-likelihood ratio test yielded a χ2 value of 0.85 with 3 degrees of freedom (p = 0.55), suggesting that the model did not significantly improve fit compared to a null model.

Statistical analysis. All analyses were conducted in Python 3.10, utilizing key libraries such as pandas for data manipulation, lifelines for survival modeling, and matplotlib for visualization. This computational environment ensured reproducibility and efficient handling of clinical and survival data from TCGA.

Results

The Fig. 1 presents a comparative analysis of hypoxia levels across tumor stages using three established hypoxia scoring systems [28–31]: Buffa, Ragnum, and Winter. Each boxplot illustrates the distribution of scores for tumor stages ranging from Stage I through Stage IV, including intermediate substages (e.g., IIA, IIIB) and a miscella- neous group labeled Stage X. This comparison provides insights into how hypoxia, a critical factor influencing tumor aggressiveness and treatment resistance, varies with tumor progression. The Buffa hypoxia score (Fig. 1A) shows considerable variabil- ity across tumor stages. Notably, intermediate stages such as IIA and IIB display elevated median scores with broader interquartile ranges, suggesting increased and heterogeneous hypoxia in these groups. In contrast, early stages like IA and IB tend to have more negative median values, indicating relatively lower hypoxia. Interestingly, Stage IIIC and Stage IV, despite being advanced, do not show a consistent increase in hypoxia scores, implying that hypoxia does not linearly correlate with tumor stage under the Buffa scoring system. The presence of

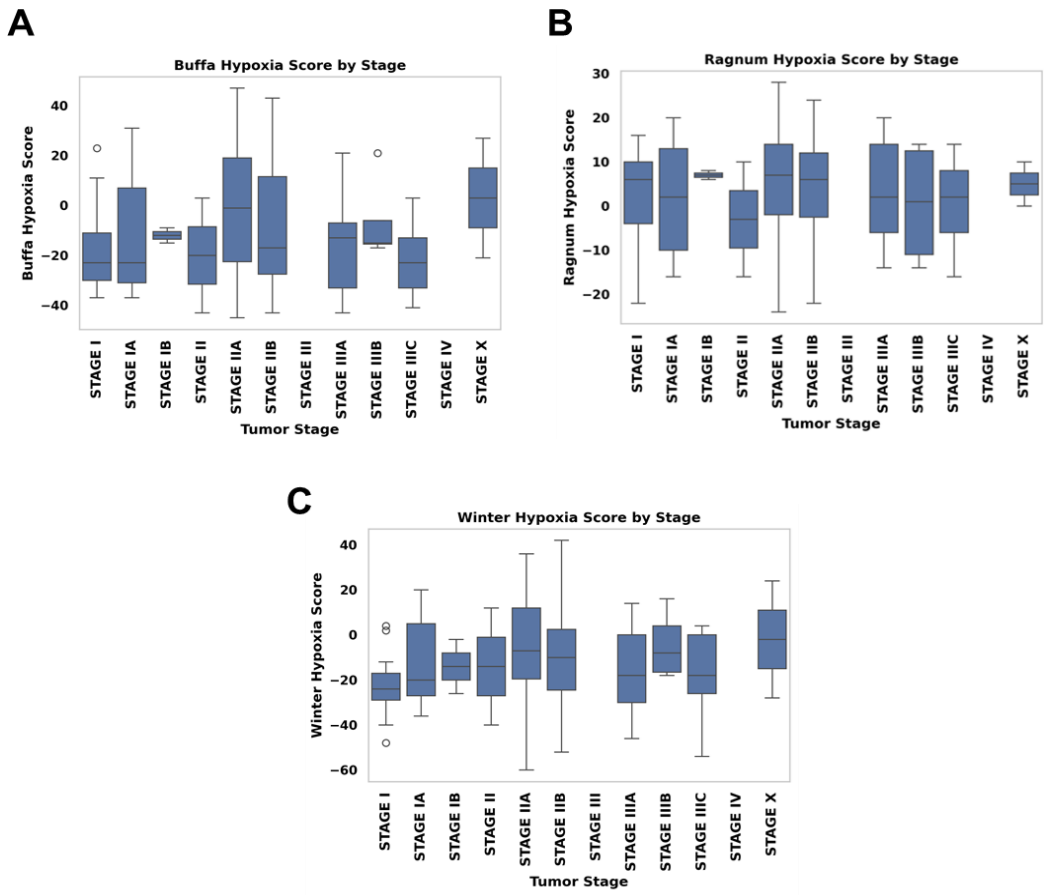


Figure 1 Hypoxia dynamics across tumor stages vary by scoring method. (A) Buffa score: Elevated hypoxia (↑ medians, broad IQRs) in intermediate stages (IIA-IIB) versus lower early stages (IA-IB); advanced stages (IIIC-IV) lack linear progression. Outliers reflect inter-patient heterogeneity- ity. **(B) Ragnum score:** Stable, moderate hypoxia (positive medians) across stages, with minimal variability in IB. **(C) Winter score:** Hypoxia ↑ in IIA-IIB and IV; early stages (I-IA) show lower scores with high variability.

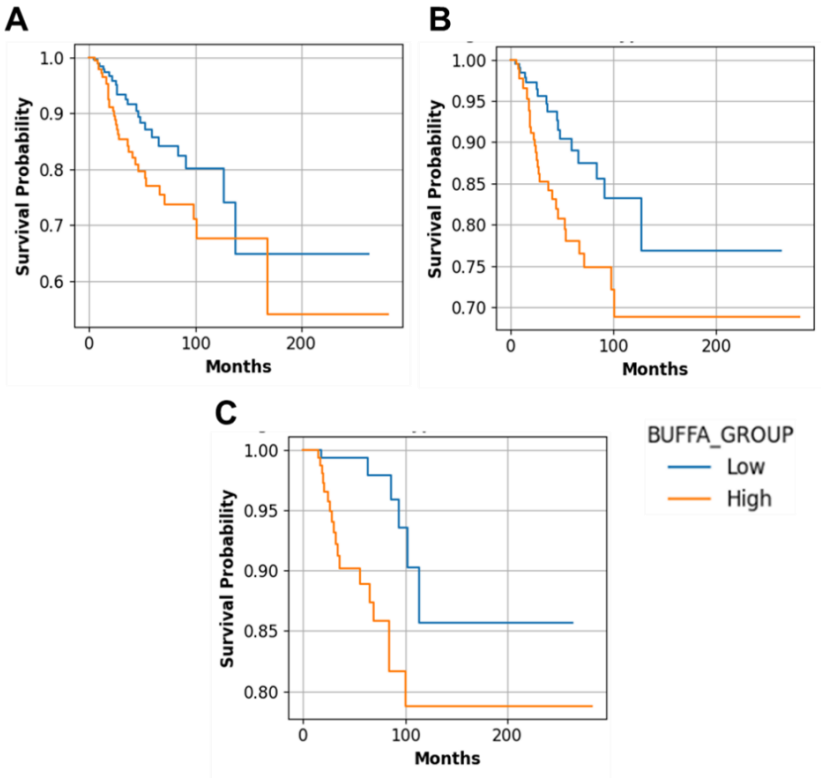


Figure. 2 Kaplan-Meier survival curves comparing High vs. Low BUFFA hypoxia score groups across three outcomes: (A) Progression-Free Survival (PFS), (B) Disease-Free Survival (DFS), and (C) Disease-Specific Survival (DSS). In each panel, survival probability is plotted against time in months. The high hypoxia group is associated with worse survival in all metrics, despite no group reaching a defined median survival.

outliers, particularly in early and intermediate stages, also reflects inter-patient heterogeneity in hypoxic response. The Ragnum hypoxia score (Fig. 1B) presents a more constrained distribution, with scores largely concentrated in the positive range across most stages. This indicates generally moderate levels of hypoxia throughout tumor progression. Stage IA and IIA stand out with slightly higher median scores, while Stage IB demonstrates minimal variability, potentially due to a smaller sample size or consistent tumor characteristics in that group. Unlike the Buffa score, the Ragnum score suggests a more stable hypoxic pro- file across stages, without marked elevation in advanced tumors. The Winter hypoxia score (Fig. 1C), which measures hypoxia on a wider scale, reveals significantly neg- ative scores in early stages such as I and IA, supporting the notion of lower oxygen deprivation in early tumor development. In contrast, intermediate stages IIA and IIB again exhibit a shift toward higher hypoxia, similar to the pattern observed in the Buffa score. Stage IV also shows increased median scores, suggesting heightened hypoxic stress in late-stage tumors. However, this pattern is accompanied by substantial variability and the presence of outliers, especially in early-stage tumors. Overall, the analysis indicates that tumor hypoxia tends to rise in intermediate to late stages of cancer progression, with notable variability depending on the scoring method. While Buffa and Winter scores highlight increased hypoxia in stages IIA and IIB, Ragnum scores suggest a more consistent, moderate hypoxic profile across all stages. These findings underscore the complexity of tumor hypoxia and the importance of considering multiple scoring approaches to capture its dynamic nature across tumor evolution[32? ? ?]

Prognostic Value of BUFFA Hypoxia Score in PFS, DFS, and DSS Survival Outcomes. The prognostic impact of the BUFFA hypoxia score (categorized as High vs. Low) was assessed across three survival metrics: progression-free survival (PFS) (Fig. 2A), disease-free survival (DFS) (Fig. 2B), and disease-specific survival (DSS) (Fig. 2C). In all three Kaplan-Meier analyses, patients in the ”High” hypoxia group demonstrated

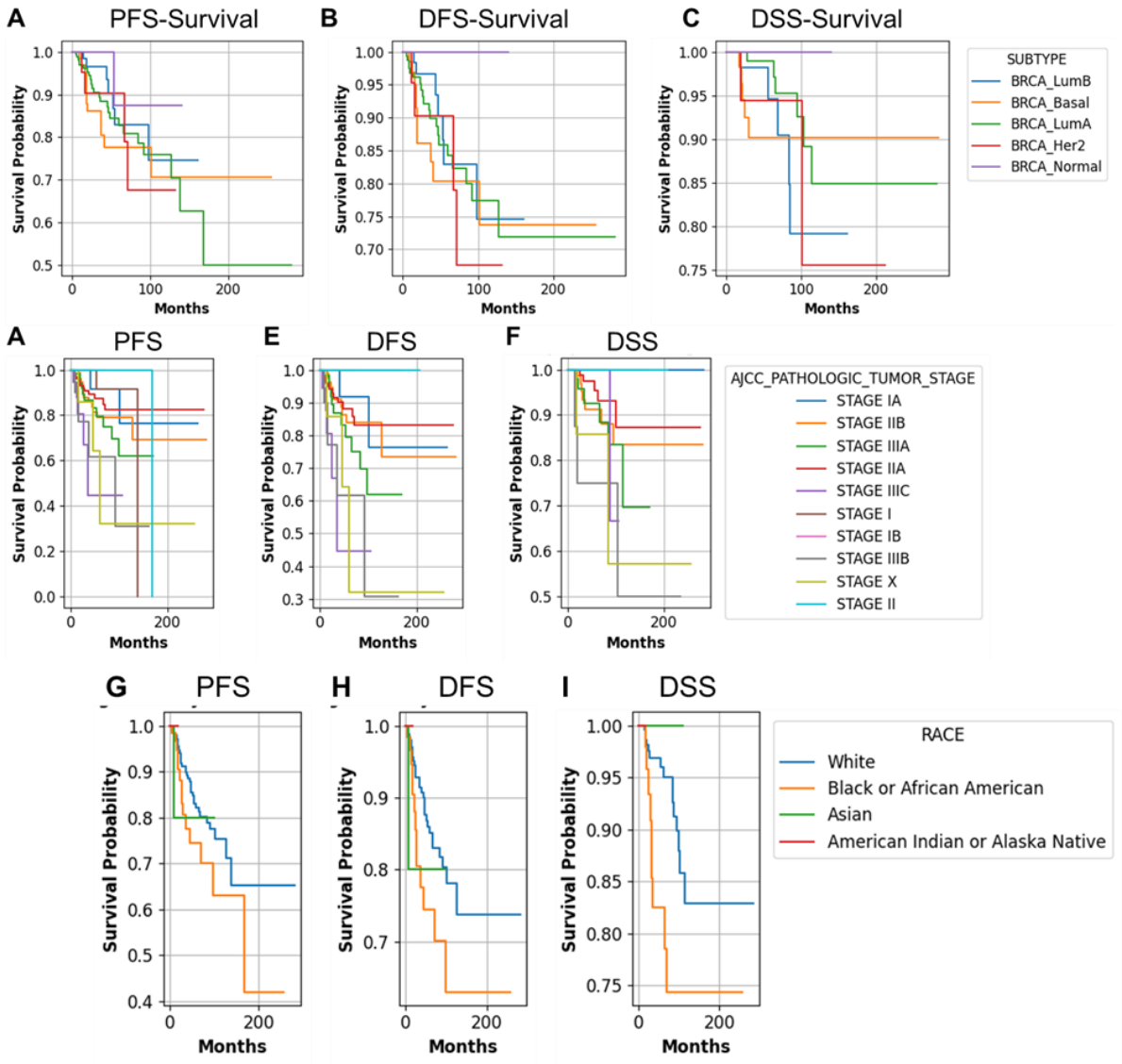


Figure. 3 Kaplan-Meier survival curves illustrating breast cancer patient outcomes across clinical stratifications. (A–C): PFS, DFS, and DSS by molecular subtype (LumA, LumB, Basal, Her2-enriched, Normal-like). (D–F): PFS, DFS, and DSS by AJCC pathologic tumor stage. (G–I): PFS, DFS, and DSS by race (White, Black or African American, Asian, American Indian or Alaska Native). All plots display survival probabilities over time in months. Most groups did not reach a median survival time ("inf"), reflecting censored observations and a favorable prognosis. Differences in event rates suggest prognostic stratification potential based on subtype, stage, and race.

reduced survival probability compared to those in the "Low" hypoxia group. For PFS, the high hypoxia group included 209 patients with 33 events, while the low group had 212 patients with 22 events. Both groups had an undefined median survival time, indicating a substantial proportion of censored data. In DFS, the high group had 31 events among 209 patients, while the low group had 17 events among 212 patients, again with no median survival reached. In the DSS comparison, the disparity was more pronounced with 18 events in the high group and only 6 in the low group, sug- gesting better disease-specific outcomes in patients with lower hypoxia scores. Overall, elevated BUFFA hypoxia scores appear to be associated with poorer outcomes across all survival endpoints, reinforcing the clinical utility of tumor hypoxia as a prognostic marker.

Prognostic Stratification of Breast Cancer Patients by Molecular Subtype, Tumor Stage, and Race Across Survival Outcomes. To explore factors

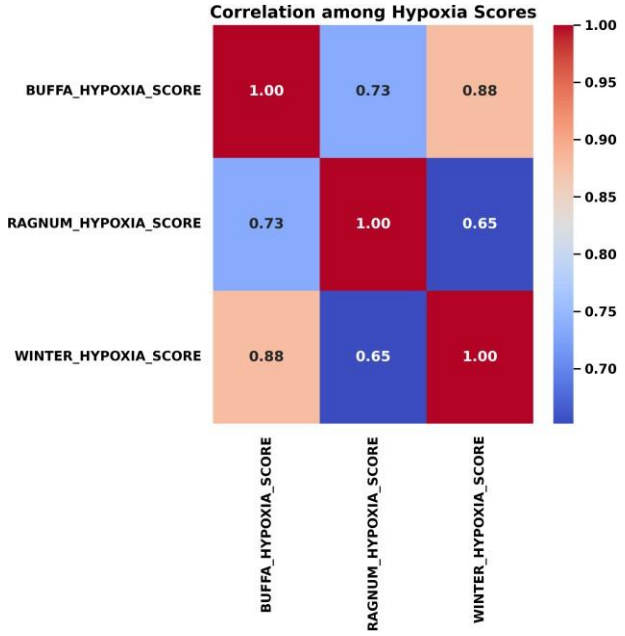


Figure. 4 Heatmap showing Pearson correlation coefficients among three hypoxia signature scores: BUFFA HYPOXIA SCORE, RAGNUM HYPOXIA SCORE, and WIN- TER HYPOXIA SCORE. All pairwise comparisons demonstrated strong positive correlations (rang- ing from 0.65 to 0.88), indicating overall consistency in hypoxia assessment across the three scoring systems

influencing breast cancer survival, we conducted Kaplan-Meier anal- yses evaluating three clinical outcomes, Progression-Free Survival (PFS), Disease-Free Survival (DFS), and Disease-Specific Survival (DSS), stratified by molecular sub- type, AJCC pathologic tumor stage, and race (Fig. 3A–3I). Subtype-specific survival analyses showed that the Luminal A (BRCA LumA) group had the largest patient population (n=180) with relatively few events (PFS: 24, DFS: 20, DSS: 6), followed by Luminal B (BRCA LumB, n = 80) and Basal-like (BRCA Basal, n = 75). All sub- types exhibited undefined median survival times across all three outcomes, indicating long-term survival and censored data. However, the Basal and Luminal B subtypes had noticeably higher event counts compared to Luminal A. HER2-enriched and Normal- like subtypes showed smaller cohorts with few events. When stratified by AJCC tumor stage, patients with earlier stages such as IA and IIA demonstrated improved survival with fewer events and undefined median survival times. In contrast, advanced stages like IIIC, IIIB, and X showed reduced survival durations—most notably Stage IIIC with a median PFS of 35.05 months and a higher event count (PFS: 5/20). This trend held across DFS and DSS metrics, reinforcing the prognostic value of clinical stag- ing. Race-based survival analysis revealed racial disparities. White patients (n=281) consistently showed favorable survival outcomes with lower event counts across all end- points. In contrast, Black or African American patients (n=64) experienced worse PFS outcomes with a median survival of 168.23 months and 14 events, suggesting potential disparities in disease progression. Asian and American Indian or Alaska Native groups had limited representation, with few events and undefined medians. These findings collectively emphasize the prognostic relevance of molecular subtype, tumor stage, and race in breast

Table. 1. Cox Proportional Hazards Model Results for Progression-Free Survival (PFS) with Age, Mutation Count, and Aneuploidy Score as Covariates.

Variable	Coef	HR (exp(coef))	SE (coef)	95% CI (HR)	z	p-value
Age	−0.00	1.00	0.02	0.96–1.03	−0.29	0.77
Mutation Count	−0.00	1.00	0.00	0.99–1.00	−0.67	0.50
Aneuploidy Score	−0.01	0.99	0.03	0.94–1.05	−0.19	0.85

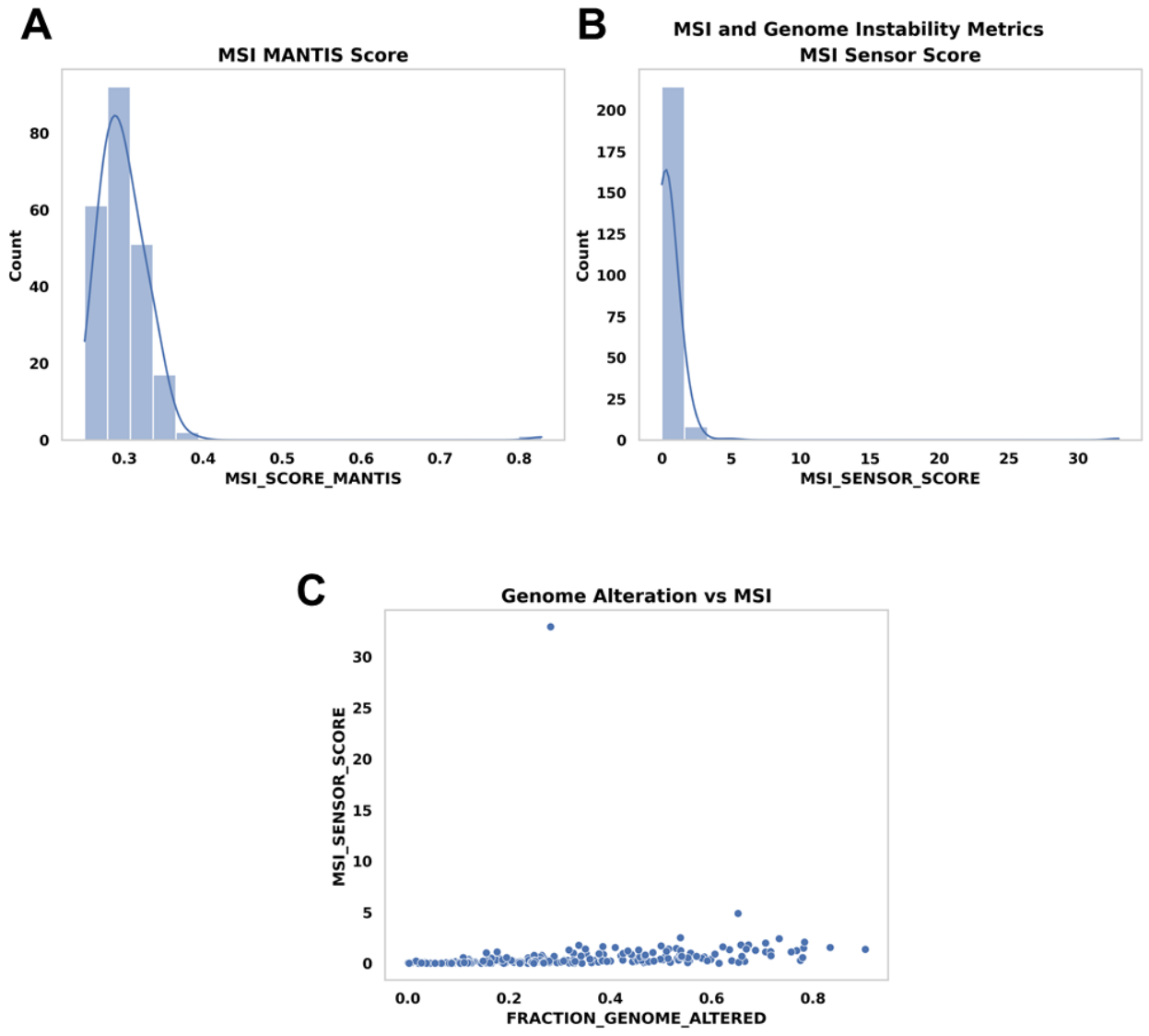


Figure. 5 Microsatellite Instability (MSI) Scores and Genome Alteration Correlation. (A) Histogram displaying the distribution of MSI MANTIS scores across samples. (B) Histogram showing the distribution of MSI Sensor scores, with a sharp peak at low values and a few high outliers. (C) Scatter plot depicting the relationship between genome instability (Fraction Genome Altered) and MSI Sensor score, highlighting a subset of samples with high instability and MSI.

cancer, supporting their use in personalized risk stratification.

Concordance Between Hypoxia Signature Scores in Breast Cancer Cohort. To evaluate the consistency among widely used hypoxia gene expression signa- tures, we computed Pearson correlation coefficients across three hypoxia scor- ing methods, Buffa, Ragnum, and Winter applied to the breast cancer cohort (Fig. 4 4). The analysis revealed strong positive correlations among all three scores, indicating that they capture overlapping yet distinct dimensions of tumor hypoxia. The BUFFA HYPOXIA SCORE showed a high correlation with the WIN- TER HYPOXIA SCORE (r = 0.88), suggesting a strong agreement in hypoxia classification between these two methods. The correlation between BUFFA and RAG- NUM scores was moderately strong (r = 0.73), while the RAGNUM and WINTER scores exhibited a slightly lower correlation (r = 0.65), though still substantial. These results imply that while all three hypoxia signatures are positively associated, the Buffa and Winter scores are more closely aligned in this dataset. This cross-signature concordance [36] supports the robustness of hypoxia profiling in breast cancer and suggests that integrating

or selecting among these scoring systems may depend on the specific biological or clinical context being investigated.

Microsatellite Instability (MSI) Scores and Genome Alteration Correlation. In Fig. 5, we evaluated microsatellite instability using two established scoring systems, MANTIS and MSI Sensor—and examined their relationship with genome alteration. Panel A shows the distribution of MSI MANTIS scores across the cohort. The majority of samples exhibit low MSI MANTIS scores, centered around 0.3, indicating a gener- ally microsatellite-stable (MSS) population. Panel B presents the distribution of MSI Sensor scores, which demonstrates a similar trend with most values concentrated near zero, although a few outliers show elevated scores, suggestive of microsatellite insta- bility (MSI-high) in select cases. Panel C explores the relationship between genomic instability and MSI, as measured by plotting the MSI Sensor Score against the Frac- tion Genome Altered. While most samples cluster at low MSI Sensor scores and low genome alteration fractions, a few samples exhibit both high MSI Sensor scores and increased genome alterations, indicating a potential link between MSI and broader genomic instability in those cases.

Cox Proportional Hazards Model for Progression-Free Survival. We performed a Cox proportional hazards [37–39] regression analysis to evaluate the association between clinical and genomic features and progression-free survival (PFS) using the lifelines.CoxPHFitter model [40]. The analysis included 224 observa- tions, of which 25 experienced a PFS event. The covariates analyzed were age, total mutation count, and aneuploidy score. None of the variables showed statistically sig- nificant associations with PFS ($p - values > 0.05$). Age and mutation count had near-zero coefficients with hazard ratios (exp(coef)) close to 1, suggesting negligible effects on risk. The aneuploidy score also demonstrated a weak negative association (coef = −0.01, HR = 0.99), though not statistically significant ($p = 0.85$). The over- all model fit, measured by partial AIC, was 227.25, and the concordance index was 0.47, indicating limited predictive power. The log-likelihood ratio test was not signif- icant ($\chi 2 = 0.85$, df = 3, $p = 0.55$), further supporting the lack of strong predictive variables in the model.

Discussion

Our analysis offers a detailed portrayal of hypoxia variation [30, 41, 42] across tumor stages and underscores the differential performance of hypoxia scoring methods in cap- turing these dynamics. The Buffa hypoxia score demonstrated the greatest variability among stages, with a clear elevation in intermediate stages (IIA and IIB), highlighting a potential window during tumor evolution where hypoxic stress intensifies. Interest- ingly, advanced stages such as IIIC and IV did not uniformly exhibit higher hypoxia levels, challenging the assumption that hypoxia linearly escalates with tumor stage. These findings suggest a complex interplay between tumor growth, angiogenesis, and local oxygen demand that may vary depending on tumor biology and microenviron- mental context. The Ragnum score [43, 44], in contrast, presented a more uniform hypoxia profile across all stages, with moderate and stable values. This scoring system may be less sensitive to subtle changes in hypoxia during progression or may reflect a gene set that is activated more broadly in solid tumors regardless of stage. Meanwhile, the Winter score partially mirrored Buffa's pattern, with higher scores in intermedi- ate and late stages, although again, variability and outlier presence especially in early

stages point to significant inter-tumoral heterogeneity [45–47]. Collectively, these com- parisons emphasize the need for multi-metric evaluation when interpreting hypoxia in breast tumors. The prognostic significance of hypoxia was particularly evident in the Buffa score analysis. Across all three survival outcomes—progression-free survival (PFS), disease-free survival (DFS), and disease-specific survival (DSS) patients in the high hypoxia group consistently exhibited worse outcomes. Although median sur- vival was not reached in most groups, the higher event counts and visibly separated Kaplan-Meier curves reinforce the role of hypoxia as an adverse prognostic indicator. These results align with the broader literature [6, 48–52], which identifies hypoxia as a contributor to treatment resistance and tumor aggressiveness. When examining clinical stratifications, molecular subtype emerged as a strong determinant of out- come. As expected, Luminal A patients had the best prognosis, with relatively few events and long survival, while Basal-like and Luminal B subtypes experienced poorer outcomes. These differences likely reflect intrinsic biological variations [53–55], such as proliferative capacity, immune response, and therapeutic responsiveness. Similarly, staging analysis reaffirmed the clinical utility of AJCC classifications, with advanced stages correlating with poorer survival. Notably, Stage IIIC consistently had shorter survival durations across all outcomes, underscoring the need for aggressive manage- ment in this group. Racial disparities also

became evident, particularly for Black or African American patients who experienced worse PFS despite similar clinical stag- ing, suggesting potential systemic differences in tumor biology, healthcare access, or comorbidity burden. This finding highlights the importance of incorporating demo- graphic and social determinants into prognostic models. The observed strong positive correlations between hypoxia scores further validate their utility, with Buffa and Win- ter showing the highest concordance. This suggests that despite their unique gene compositions, these signatures largely capture similar hypoxia-related biological pro- cesses. However, the modest discrepancy between Ragnum and the other two scores suggests that certain gene sets may respond differently to hypoxic stress or reflect distinct temporal windows of oxygen deprivation. Lastly, our evaluation of MSI using MANTIS and MSI Sensor revealed a predominantly microsatellite-stable cohort, with a few outliers indicating possible MSI-high tumors. A subset of samples showed con- current high MSI Sensor scores and elevated genome alterations, suggesting that, in some cases, MSI may contribute to broader genomic instability [56–59]. However, the rarity of these cases in breast cancer supports existing knowledge that MSI is less prevalent [61?] in this tumor type compared to colorectal or endometrial cancers.

In conclusion, this integrative analysis highlights the heterogeneity and prognostic significance of tumor hypoxia in breast cancer. While intermediate stages exhibit heightened hypoxia in some scoring systems, overall survival outcomes are consistently worse in hypoxic tumors. These findings underscore the value of combining multiple hypoxia metrics with clinical and molecular stratifiers to refine prognostic assessments and inform targeted interventions.

Conflict of interest

None to declare.

Acknowledgment and funding

None

References

1. Ruan K, Song G, Ouyang G. Role of hypoxia in the hallmarks of human cancer. J Cell Biochem. 2009; 107: 1053-62. [PubMed] [Google Scholar]
2. Sarkar M, Niranjan N, Banyal PK. Mechanisms of hypoxemia. Lung India. 2017; 34: 47-60. [PubMed] [Google Scholar]
3. Semenza GL. The hypoxic tumor microenvironment: A driving force for breast cancer progression. Biochim Biophys Acta. 2016; 1863: 382-91. [PubMed] [Google Scholar]
4. Boudreau N, Myers C. Breast cancer-induced angiogenesis: multiple mechanisms and the role of the microenvironment. Breast Cancer Res. 2003, 5, 1–7. [PubMed] [Google Scholar]
5. Wang M, Zhang C, Song Y, Wang Z, Wang Y, Luo F, Xu Y, Zhao Y, Wu Z, Xu Y. Mechanism of immune evasion in breast cancer. Onco Targets Ther. 2017 Mar 14; 10: 1561–73. [PubMed] [Google Scholar]
6. Jing X, Yang F, Shao C, Wei K, Xie M, Shen H, Shu Y. Role of hypoxia in cancer therapy by regulating the tumor microenvironment. Mol Cancer. 2019; 18: 157: 1–15. [PubMed] [Google Scholar]
7. Zeng J, Wang J, Gao W, Mohammadreza A, Kelbauskas L, Zhang W, Johnson RH, Meldrum DR. Quantitative single-cell gene expression measurements of multiple genes in response to hypoxia treatment. Anal Bioanal Chem. 2011; 401:3-13. [PubMed] [Google Scholar]
8. Badowska-Kozakiewicz AM, Budzik MP, Przybylski J. Hypoxia in breast cancer. Pol J Pathol. 2015; 66: 337-46. [PubMed] [Google Scholar]
9. Bracken, C., Whitelaw, M., Peet, D. The hypoxia-inducible factors: Key tran-scriptional regulators of hypoxic responses. Cellular and Molecular Life Sciences (CMLS) 2003, 60, 1376–93. [PubMed] [Google Scholar]
10. Dengler, V.L., Galbraith, M.D., Espinosa, J.M. Transcriptional regulation by hypoxia inducible factors. Critical Reviews in Biochemistry and Molecular Biology 2014, 49, 1–15. [PubMed] [Google Scholar]
11. Liu L, Simon MC. Regulation of transcription and translation by hypoxia. Cancer Biol Ther. 2004 Jun;3(6):492-7. [PubMed] [Google Scholar]
12. Khan SU, Ullah Z, Shaukat H, Unab S, Jannat S, Ali W, Ali A, Irfan M, Khan MF, Cervantes-Villagrana RD. TP53 and its Regulatory Genes as Prognosis of Cutaneous Melanoma. Cancer Inform 2023; 22: 11769351231177267. [PubMed] [Google Scholar]
13. Haensgen G, Krause U, Becker A, Stadler P, Lautenschlaeger C, Wohlrab W, Rath FW, Molls M, Dunst J. Tumor hypoxia, p53, and prognosis in cervical cancers. Int J Radiat Oncol Biol Phys. 2001; 50: 865-72. [PubMed] [Google Scholar]
14. Regazzetti C, Peraldi P, Grémeaux T, Najem-Lendom R, Ben-Sahra I, Cormont M, Bost F, Le Marchand-Brustel Y, Tanti JF, Giorgetti-Peraldi S. Hypoxia decreases insulin signaling pathways in adipocytes. Diabetes. 2009; 58:95-103. [PubMed] [Google Scholar]
15. Alyas J, Rafiq A, Amir H, Khan SU, Sultana T, Ali A, Hameed A, Ahmad I, Kazmi A, Sajid TJBR. Human insulin: History, recent advances, and expression systems for mass production. Biomed Res Ther. 2021, 8, 4540–4561. [Google Scholar]

16. Khan SU, Jannat S, Shaukat H, Unab S, Tanzeela, Akram M, Khan Khattak MN, Soto MV, Khan MF, Ali A, Rizvi SSR. Stress Induced Cortisol Release Depresses The Secretion of Testosterone in Patients With Type 2 Diabetes Mellitus. Clin Med Insights Endocrinol Diabetes. 2023; 16: 11795514221145841. [PubMed] [Google Scholar]
17. Khan SU, Akram M, Iqbal Z, Javid M, Unab S, Jannat S, Ali A, Khan MF, Ali W, Rafi MJRJoDN, Diseases M. 2022. Relationship between testosterone and cortisol levels and body mass index in men with type 2 diabetes mellitus. 29:341-348. [Google Scholar]
18. Ullah Khan S, Daniela Hernández-González K, Ali A, Shakeel Raza Rizvi S. Diabetes and the fabkin complex: A dual-edged sword. Biochem Pharmacol. 2024; 223: 116196. [PubMed] [Google Scholar]
19. Catrina, S.-B., Zheng, X. Hypoxia and hypoxia-inducible factors in diabetes and its complications. Diabetologia 2021, 64, 709–716. [PubMed] [Google Scholar]
20. Javid M, Khan SU, Akram M, Cervantes-Villagrana RD, Rafi M, Khan MF, Raza Rizvi SS. Higher cortisol level and reduced circulating triiodothyronine in patients with cardiovascular diseases: A case-control study. JRSM Cardiovasc Dis. 2025, 14, 20480040251340609. [PubMed] [Google Scholar]
21. Giussani, D.A. Breath of life: Heart disease link to developmental hypoxia. Circulation 2021, 144, 1429–43. [PubMed] [Google Scholar]
22. Rabalais, N., Diaz, R.J., Levin, L., Turner, R.E., Gilbert, D., Zhang, J. Dynamics and distribution of natural and human-caused hypoxia. Biogeosciences 2010, 7, 585–619. [Google Scholar]
23. Saxena, K., Jolly, M.K. Acute vs. chronic vs. cyclic hypoxia: Their differential dynamics, molecular mechanisms, and effects on tumor progression. Biomolecules 2019, 9, 339. [PubMed] [Google Scholar]
24. Ali A, Mashwani ZU, Ahmad I, Raja NI, Mohammad S, Khan SU. Plant in vitro cultures: A promising and emerging technology for the feasible production of antidiabetic metabolites in Caralluma tuberculata. Front Endocrinol (Lausanne). 2022, 13, 1029942. [PubMed] [Google Scholar]
25. Aravinth A, Dhanasundaram S, Perumal P, Kamaraj C, Khan SU, Ali A, Ragavendran C, Amutha V, Rajaram R, Santhanam P, Luna-Arias JP, Mashwani ZU. Evaluation of Brown and red seaweeds-extracts as a novel larvicidal agent against the deadly human diseases-vectors, Anopheles stephensi, Aedes aegypti and Culex quinquefasciatus. Exp Parasitol. 2024, 256, 108651. [PubMed] [Google Scholar]
26. Iftikhar F, Qureshi R, Siddiqa A, Anwar K, Arshad F, Mashwani Z-U-R, Riaz A, Khan SU, Ali A, Iqbal SJCJoFS. Harnessing nature's secrets: Silver nanoparticles from Withania coagulans fruit and root extracts unveil exceptional antioxidant and antimicrobial properties. Czech Journal of Food Sciences 2024,42, 192–206. [Google Scholar]
27. Murugesan S, Ragavendran C, Ali A, Arumugam V, Lakshmanan DK, Palanichamy P, Venkatesan M, Kamaraj C, Luna-Arias JP, Fabián F-LJIJoTM. Screening and druggability analysis of marine active metabolites against SARS-CoV-2: An integrative computational approach. International Journal of Translational Medicine 2022, 3, 27–41. [Google Scholar]
28. Thompson CM, Puterman AS, Linley LL, Hann FM, van der Elst CW, Molteno CD, Malan AF. The value of a scoring system for hypoxic ischaemic encephalopathy in predicting neurodevelopmental outcome. Acta Paediatr. 1997, 86, 757–761. [PubMed] [Google Scholar]
29. Arjun R, Acharya S, Shender BS, Rorres C, Hrebien L, Kam M. Correlation of Cognitive Scores and the Onset of Hypoxia. Aerosp Med Hum Perform. 2019, 90, 429–39. [PubMed] [Google Scholar]
30. Jubb, A.M., Buffa, F.M., Harris, A.L. Assessment of tumour hypoxia for prediction of response to therapy and cancer prognosis. Journal of Cellular and Molecular Medicine 2010, 14, 18–29. [PubMed] [Google Scholar]
31. Liu Z, Tang Q, Qi T, Othmane B, Yang Z, Chen J, Hu J, Zu X. A Robust Hypoxia Risk Score Predicts the Clinical Outcomes and Tumor Microenvironment Immune Characters in Bladder Cancer. Front Immunol. 2021, 12, 725223. [PubMed] [Google Scholar]
32. McGranahan, N., Swanton, C. Clonal heterogeneity and tumor evolution: Past, present, and the future. Cell 2017, 168, 613–28. [PubMed] [Google Scholar]
33. Amirouchene-Angelozzi, N., Swanton, C., Bardelli, A. Tumor evolution as a therapeutic target. Cancer Discovery 2017, 7, 805–17. [PubMed] [Google Scholar]
34. Galon, J., Bruni, D. Tumor immunology and tumor evolution: Intertwined histories. Immunity 2020, 52, 55–81. [PubMed] [Google Scholar]
35. Lorusso, G., Ru¨egg, C. The tumor microenvironment and its contribution to tumor evolution toward metastasis. Histochemistry and Cell Biology 2008, 130, 1091–103. [PubMed] [Google Scholar]
36. Graham NA, Minasyan A, Lomova A, Cass A, Balanis NG, Friedman M, Chan S, Zhao S, Delgado A, Go J, Beck L, Hurtz C, Ng C, Qiao R, Ten Hoeve J, Palaskas N, Wu H, Müschen M, Multani AS, Port E, Larson SM, Schultz N, Braas D, Christofk HR, Mellinghoff IK, Graeber TG. Recurrent patterns of DNA copy number alterations in tumors reflect metabolic selection pressures. Mol Syst Biol. 2017, 13, 914. [PubMed] [Google Scholar]
37. Broglio KR, Berry DA. Detecting an overall survival benefit that is derived from progression-free survival. J Natl Cancer Inst. 2009, 101, 1642–9. [PubMed] [Google Scholar]
38. Halabi, S., Vogelzang, N.J., Ou, S.-S., Owzar, K., Archer, L., Small, E.J. Progression-free survival as a predictor of overall survival in men with castrate-resistant prostate cancer. Journal of Clinical Oncology 2009, 27, 2766–71. [PubMed] [Google Scholar]
39. Fleischer, F., Gaschler-Markefski, B., Bluhmki, E. A statistical model for the dependence between progression-free survival and overall survival. Statistics in Medicine 2009, 28, 2669–86. [PubMed] [Google Scholar]
40. Araldi, E., Jutzeler, C.R., Ristow, M. Lithium treatment extends human lifespan: Findings from the UK Biobank. Aging (Albany NY) 2023, 15, 421. [PubMed] [Google Scholar]
41. Bader, S.B., Dewhirst, M.W., Hammond, E.M. Cyclic hypoxia: An update on its

characteristics, methods to measure it and biological implications in cancer. Cancers 2020, 13, 23. [PubMed] [Google Scholar]

42. Chi JT, Wang Z, Nuyten DS, Rodriguez EH, Schaner ME, Salim A, Wang Y, Kristensen GB, Helland A, Børresen-Dale AL, Giaccia A, Longaker MT, Hastie T, Yang GP, van de Vijver MJ, Brown PO. Gene expression programs in response to hypoxia: cell type specificity and prognostic significance in human cancers. PLoS Med. 2006, 3, e47. [PubMed] [Google Scholar]
43. Ragnum HB, Vlatkovic L, Lie AK, Axcrona K, Julin CH, Frikstad KM, Hole KH, Seierstad T, Lyng H. The tumour hypoxia marker pimonidazole reflects a transcriptional programme associated with aggressive prostate cancer. Br J Cancer. 2015, 112, 382–90. [PubMed] [Google Scholar]
44. Ragnum HB, Røe K, Holm R, Vlatkovic L, Nesland JM, Aarnes EK, Ree AH, Flatmark K, Seierstad T, Lilleby W, Lyng H. Hypoxia-independent downregulation of hypoxia-inducible factor 1 targets by androgen deprivation therapy in prostate cancer. Int J Radiat Oncol Biol Phys.2013, 87, 753–60. [PubMed] [Google Scholar]
45. Torrecilla S, Sia D, Harrington AN, Zhang Z, Cabellos L, Cornella H, Moeini A, Camprecios G, Leow WQ, Fiel MI, Hao K, Bassaganyas L, Mahajan M, Thung SN, Villanueva A, Florman S, Schwartz ME, Llovet JM. Trunk mutational events present minimal intra- and inter-tumoral heterogeneity in hepatocellular carcinoma. J Hepatol. 2017, 67, 1222–31. [PubMed] [Google Scholar]
46. Jeantet M, Tougeron D, Tachon G, Cortes U, Archambaut C, Fromont G, Karayan-Tapon L. High Intra- and Inter-Tumoral Heterogeneity of RAS Mutations in Colorectal Cancer. Int J Mol Sci. 2016, 17, 2015. [PubMed] [Google Scholar]
47. Chiu AM, Mitra M, Boymoushakian L, Coller HA. Integrative analysis of the inter-tumoral heterogeneity of triple-negative breast cancer. Sci Rep. 2018, 8, 11807. [PubMed] [Google Scholar]
48. Vaupel P. Hypoxia and aggressive tumor phenotype: implications for therapy and prognosis. Oncologist. 2008, 13, 21–6. [PubMed] [Google Scholar]
49. Muz, B., De La Puente, P., Azab, F., Kareem Azab, A. The role of hypoxia in cancer progression, angiogenesis, metastasis, and resistance to therapy. Hypoxia 2015, 83–92. [PubMed] [Google Scholar]
50. Karakashev SV, Reginato MJ. Progress toward overcoming hypoxia-induced resistance to solid tumor therapy. Cancer Manag Res. 2015, 253– 64. [PubMed] [Google Scholar]
51. Vaupel P. The role of hypoxia-induced factors in tumor progression. Oncologist. 2004, 9, 10–7. [PubMed] [Google Scholar]
52. Vasseur, S., Tomasini, R., Tournaire, R., Iovanna, J.L. Hypoxia induced tumor metabolic switch contributes to pancreatic cancer aggressiveness. Cancers 2010, 2, 2138–52. [PubMed] [Google Scholar]
53. Wu S, Zhu W, Thompson P, Hannun YA. Evaluating intrinsic and non-intrinsic cancer risk factors. Nat Commun. 2018, 9, 3490. [PubMed] [Google Scholar]
54. Sun XX, Yu Q. Intra-tumor heterogeneity of cancer cells and its implications for cancer treatment. Acta Pharmacol Sin. 2015, 36, 1219–27. [PubMed] [Google Scholar]
55. Yuan R, Zhu X, Wang G, Li S, Ao P. Cancer as robust intrinsic state shaped by evolution: a key issues review. Rep Prog Phys. 2017, 80, 042701. [PubMed] [Google Scholar]
56. Abbas T, Keaton MA, Dutta A. Genomic instability in cancer. Cold Spring Harb Perspect Biol. 2013, 5, a012914. [PubMed] [Google Scholar]
57. Charames GS, Bapat B. Genomic instability and cancer. Curr Mol Med. 2003, 3, 589–97. [PubMed] [Google Scholar]
58. Yao Y, Dai W. Genomic Instability and Cancer. J Carcinog Mutagen. 2014, 5, 1000165. [PubMed] [Google Scholar]
59. Shen, Z. Genomic Instability and Cancer: An Introduction. Oxford University Press: 2011; Vol. 3, pp. 1–3. [Google Scholar]
60. Halford SE, Sawyer EJ, Lambros MB, Gorman P, Macdonald ND, Talbot IC, Foulkes WD, Gillett CE, Barnes DM, Akslen LA, Lee K, Jacobs IJ, Hanby AM, Ganesan TS, Salvesen HB, Bodmer WF, Tomlinson IP, Roylance RR. MSI-low, a real phenomenon which varies in frequency among cancer types. J Pathol. 2003, 201, 389–94. [PubMed] [Google Scholar]
61. Ashktorab H, Ahuja S, Kannan L, Llor X, Ellis NA, Xicola RM, Laiyemo AO, Carethers JM, Brim H, Nouraie M. A meta-analysis of MSI frequency and race in colorectal cancer. Oncotarget. 2016, 7, 34546. [PubMed] [Google Scholar]

How to cite this article. Migabo EM, Mwata-Velu T, Mavuela-Maniansa R, Milomba Velu R, Tshibangu-Mbuebue B, Angoma-Shindani B, Yaseen N, Mbungu Baptista A. Multi-dimensional assessment of tumor hypoxia, survival outcomes, and molecular stratification in breast cancer using computational skills. ***Avan Biomed*** 2025; 14: 149-60.

Avances en Biomedicina se distribuye bajo la Licencia CreativeCommons Atribución-NoComercial-CompartirIgual 4. 0 Venezuela, por lo que el envío y la publicación de artículos a la revista son completamente gratuitos.

https://q.me-qr.com/aNfwV0g3